J|A|C|S ARTICLES

Published on Web 10/29/2009

Room-Temperature Synthesis of Soluble Carbon Nanotubes by the Sonication of Graphene Oxide Nanosheets

Shuai Wang,[†] Lena Ai ling Tang,[†] Qiaoliang Bao,[†] Ming Lin,[‡] Suzi Deng,[†] Bee Min Goh,[†] and Kian Ping Loh*,[†]

Department of Chemistry, National University of Singapore, 3 Science Drive 3, 117543 Singapore, and Institute of Materials Research and Engineering, 3 Research Link, S11760 Singapore

Received July 17, 2009; E-mail: chmlohkp@nus.edu.sg

Abstract: The transformation of two-dimensional graphene oxide (GO) nanosheets into carbon nanotubes was achieved by sonicating GO in 70% nitric acid. Through the use of mass spectrometry to track the evolution of molecular fragments during the acid ultrasonication, it was observed that GO can be readily decomposed into polyaromatic hydrocarbons (PAHs). The cavitation-induced condensation of these PAHs results in their molecular reconstruction to form folded carbon nanostructures. UV-emitting, water-soluble carbon nanoparticles as well as carbon nanotubes that exhibit magnetic properties were fabricated under catalyst-free conditions.

Introduction

The synthesis of low-dimensional carbon nanostructures by vaporization or chemical vapor deposition methods is effective when facile production in large quantities is concerned. However, wet chemical synthesis approaches based on rational design are of fundamental interest and present advantages in terms of the tailored synthesis of unique structures such as endohedral fullerenes, heterofullerenes, and coordination assemblies of polymers or organic−inorganic wires. A bottom-up, wet-chemistry route to the synthesis of low-dimensional carbon nanostructures is not trivial because of the intricate chemical design needed for the coupling of aryl precursors, which must then be followed by dehydrogenation and folding of any assembled structure. The rational organic synthesis of C_{60} by Scott and co-workers in 2002 involved 13 steps, and the final step required flash vacuum pyrolysis of large polycyclic aromatic hydrocarbons (PAHs) at 1100 °C.[1] In 2008, Otego and co-workers simplified and improved the yield of the process by using surface-catalyzed cyclodehydrogenation of polyaromatics having topology suitable for forming fullerenes.[2] Extending from fullerenes to one-dimensional carbon structures presents a quantum leap in the level of difficulty for wet chemical synthesis. In comparison with the tremendous amount of publications in gas-phase synthesis of carbon nanotubes (CNTs), there are limited reports on liquid-phase routes to the production of CNTs, despite the attractiveness of such approaches in terms of batch-type solution processing. Earlier attempts at liquid-phase synthesis utilized catalytic growth processes on a heated substrate (800−1000 °C) in organic solvents.[3] Even though these reactions can be controlled safely on the laboratory scale, they are not upwardly scalable because of potential hazards involved with the dissipation of heat in large volumes of volatile organic solvents. Notable advances to address these issues include the synthesis of CNTs by a modified Wolff−Kishner reduction process as well as by the catalytic decomposition of carbon tetrachloride, with temperatures as low as 180 °C.[4,5]

A unifying approach based on the use of PAHs as precursors to new carbon forms is attractive. Carbon-rich acetylenic spherical macrocylces and bowl-shaped hydrocarbons with curved networks of polyarenes have been used as precursors for the synthesis of fullerenes. The synthesis of carbon nanotubes from PAHs is challenging because it necessitates long-range assembly, dehydrogenation, and scrolling. One strategy is to apply a template-assisted method to preassemble the PAHs on a tubular scaffold. The capillary infiltration of PAH solutions into nanochannel alumina followed by solvent evaporation deposits thin organic films on inner wall surfaces, and the subsequent pyrolysis of these organic films can produce sp^2-hybridized carbon structures at high temperature.[6]

In this work, we report a catalyst-free wet chemistry route to the synthesis of fullerenes and CNTs at room temperature. The work is inspired by the structure and solubility of graphene oxide (GO), which provides the perfect scaffold for decomposition into tiny fragments of soluble PAHs in acidic condition. Whereas the PAHs generated from the incomplete pyrolysis of organic materials in vapors have very low solubility and cannot be readily processed in solution, the uniqueness of PAHs generated

[†] National University of Singapore.
[‡] Institute of Materials Research and Engineering.

(1) Scott, L. T.; Boorum, M. M.; McMahon, B. J.; Hagen, S.; Mack, J.; Blank, J.; Wegner, H.; de Meijere, A. *Science* **2002**, *295*, 1500.
(2) Otero, G.; Biddau, G.; Sánchez-Sánchez, C.; Caillard, R.; López, M. F.; Rogero, C.; Palomares, F. J.; Cabello, N.; Basanta, M.; Ortega, J.; Méndez, J.; Echavarren, A. M.; Pérez, R.; Gómez-Lor, B.; Martín-Gago, J. A. *Nature* **2008**, *454*, 865.
(3) Zhang, Y. E.; Gamo, M. N.; Nakagawa, K.; Ando, T. *J. Mater. Res.* **2002**, *17*, 2457.
(4) Vohs, J. K.; Brege, J. J.; Raymond, J. E.; Brown, A. E.; Williams, G. L.; Fahlman, B. D. *J. Am. Chem. Soc.* **2004**, *126*, 9936.
(5) Wang, W. Z.; Kunwar, S.; Huang, J. Y.; Wang, D. Z.; Ren, Z. F. *Nanotechnology* **2005**, *16*, 21.
(6) Jian, K. Q.; Shim, H.-S.; Schwartzman, A.; Crawford, G. P.; Hurt, R. H. *Adv. Mater.* **2003**, *15*, 164.

10.1021/ja905968v CCC: $40.75

from GO in an acidic environment is their solubility, which implies an applicability to synthesis.

GO nanosheets can be generated from acid oxidation and exfoliation of graphite flakes.[7] Because of the presence of negatively charged oxygenated groups like epoxy and hydroxyl on the basal planes as well as carboxylic groups decorating the edges, GO can be readily dispersed at the single-sheet level in water. GO nanosheets can be reduced to graphene upon thermal deoxidation or chemical reduction. The size of the fragmented GO sheets can be controlled by varying the sonication time. We hypothesized that sonicating GO in concentrated acids could cut the GO nanosheets into nanofragments and soluble polyaromatics, which subsequently undergo cavitation-induced condensation to form various carbon nanostrutures.

Experimental Section

Chemicals. Graphite was bought from Bay Carbon (SP-1). $NaNO_3$, H_2SO_4, $KMnO_4$, and H_2O_2 were purchased from Aldrich.

Synthesis of Graphene Oxide. A conical flask equipped with a magnetic stirring bar was charged with 69 mL of H_2SO_4 and cooled to 0−5 °C by immersion in an ice bath. Graphite (1.5 g) was then added slowly with vigorous stirring while maintaining the reaction mixture at 0−5 °C. After the added graphite flakes formed a well-dispersed black slurry, 1.5 g of $NaNO_3$ was added slowly over 15 min at 0−5 °C. The mixture was allowed to warm to room temperature (RT) and stirred for 1 h. Water (120 mL) was then added, and the solution was stirred for 30 min while the temperature was raised to 90 °C. The mixture was poured into 300 mL of water, after which 10 mL of H_2O_2 was slowly added. The color of the solution changed from dark-brown to yellow. The solution was then filtered. The material was redispersed in water and washed with water until the pH of the filtrate was neutral. The resultant GO material was dried in a vacuum desiccator overnight at RT and stored in the ambient environment.

Room-Temperature Synthesis of Soluble Carbon Nanotubes from the Sonication of Graphene Oxide Nanosheets. GO (10 mg) and 70% HNO_3 solution (10 mL) were added to a 50 mL bottle. The bottle was sealed and then sonicated in a bath sonicator at RT for 4 h (50/60 Hz). After reaction, the mixture was poured into 400 mL of water. The solution was centrifuged at 15 000 rpm to remove the acid. To purify these CNTs, the material was redispersed in 11 mL of water. The solution was added to a centrifuge tube (polycarbonate, 15 mL) and centrifuged at 12 000 rpm for 1 h, after which the first 3 mL fraction along the centrifuge tube was removed. This first fraction contained fullerene-like nanoparticles. The second 3 mL fraction that was collected contained CNTs. The precipitate (the final fraction in the centrifuge tube) contained long, flat ribbonlike tapes (nanoribbons), which were probably formed by scissoring of GO sheets along their line defects.

Synthesis of Carbon Nanoparticles from the Sonication of Graphene Oxide Nanosheets. GO (10 mg) and 70% HNO_3 solution (10 mL) were added to a 50 mL bottle. The bottle was sealed and then sonicated in bath sonicator at 60 °C for 4 h (50/60 Hz). After reaction, the mixture was poured into 400 mL of water. The solution was centrifuged at 15 000 rpm to remove the acid. The resultant material was then dried in a vacuum desiccator overnight at room temperature and stored in the ambient environment.

Characterization. Transmission electron microscopy (TEM) measurements were conducted with a JEOL 2100 microscope with an acceleration voltage of 200 kV. X-ray photoelectron spectroscopy (XPS) was performed using a Phobios 100 electron analyzer equipped with five channeltrons and a nonmonochromatized Mg Kα X-ray source (1253.6 eV). UV−vis absorption and photoluminescence (PL) spectra were recorded on a Shimadzu UV 2450PC spectrophotometer and Perkin-Elmer LS 55 luminescence spectrometer, respectively. The magnetic properties of the CNTs were measured by an alternating gradient magnetometer (AGM), with the field applied in the in-plane direction. The composition of the samples sonicated at RT for different times were analyzed using a liquid chromatography−mass spectrometry (LC−MS) instrument (Finnigan LCQ). The column was Luna 5u C18 (250 mm × 3 mm), and acetonitrile/water was used as the mobile phase. Raman spectroscopy was performed with a WITec CRM200 confocal micro-Raman system with a 488 nm excitation laser (laser spot size ∼0.5 μm) operated at a low power level (<2 mW) in order to avoid any heating effect. The CNT samples synthesized from GO were drop-cast onto a Si substrate for Raman measurements, and the Si peak at 520 cm^{-1} was used as a reference for wavenumber calibration. For comparison, purified single-walled nanotubes (SWNTs) (purchased from Sigma-Aldrich) were also measured under the same conditions.

Results and Discussion

Use of sonication in combination with strong acids is an established method for cutting SWNTs into shorter pieces.[8] The effect arises from cavitation bubbles, which generate high strain rates in the surrounding liquid upon implosion. It has been calculated that for water under ambient conditions, sonication with an ultrasound frequency of 20 kHz at an acoustic pressure of 10 bar generates a strain rate in a collapsing bubble as large as 10^9 s^{-1}.[9] Friction forces between the moving liquid stretch the carbon framework and result in bond fracture if the load is high enough. With the help of sonicating power, the action of concentrated (70%) HNO_3 consumed the edges and existing damage sites of the GO sheets, which resulted in the cutting of large GO sheets into small-sized GO fragments. Because of its two-dimensional open structure, GO can be cut into polyaromatics in 10 min of sonication at RT. In contrast, CNTs[8] require 9 h of oxidation in concentrated acids at 70 °C, where the cutting includes circumferential and axial consumption. The presence of H^+ ions results in hydrogenation of the dangling bonds generated in the cutting, ultimately decomposing the fragments into PAH molecules. It can be expected that the smaller-sized molecules should be soluble because of the presence of edge functionalities such as hydroxyl or carboxylic groups originating from the graphene oxide, but the larger-sized fragments may aggregate to become poorly organized polyaromatic amorphous carbon.

Evidence for the generation of polyaromatics from the sonication of GOs was derived from a time-dependent mass spectrometry analysis of molecular fragments obtained from the sonicated solutions of GOs after filtering away the insoluble fragments. Figure 1 shows changes in the relative abundance of small molecules at different reaction times. It must be pointed out that a baseline check with LC−MS revealed that no large molecules existed in the mixture of GO and 70% HNO_3 prior to sonication. Upon sonication, soluble polyaromatic molecules appeared, as judged from the appearance of strong peaks in the range m/z 174−254, which can be assigned to the hydroxylated analogues of naphthalene, anthracene, and pyrene existing as mixtures in the solution. Separation of these species requires quite involved chromatographic techniques and is thus outside the scope of the present investigation. Another fingerprint of

(7) Stankovich, S.; Piner, R. D.; Nguyen, S. T.; Ruoff, R. S. *Carbon* **2006**, *44*, 3342.

(8) Ziegler, K. J.; Gu, Z. N.; Peng, H. Q.; Flor, E. L.; Hauge, R. H.; Smalley, R. E. *J. Am. Chem. Soc.* **2005**, *127*, 1541.

(9) (a) Hennrich, F.; Krupke, R.; Arnold, K.; Rojas Stütz, J. A.; Lebedkin, S.; Koch, T.; Schimmel, T.; Kappes, M. M. *J. Phys. Chem. B.* **2007**, *111*, 1932. (b) Forrest, G. A.; Alexander, A. J. *J. Phys. Chem. C* **2007**, *111*, 10792.

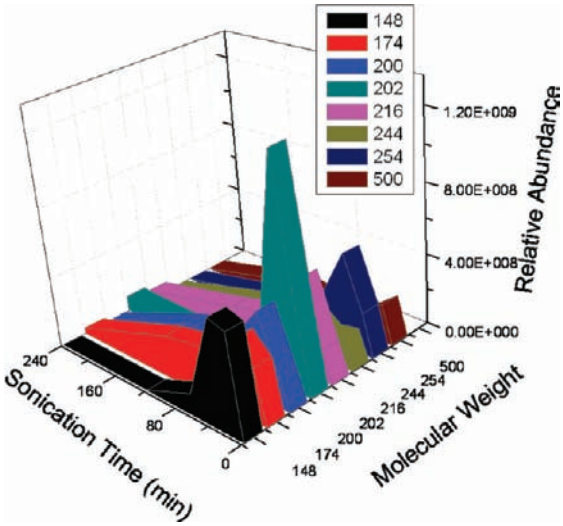

Figure 1. Mass spectra of aliquots collected from ultrasonicated GO in 70% HNO_3 plotted as a function of ultrasonication time and molecular weight.

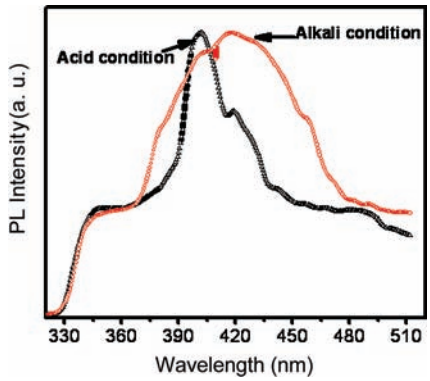

Figure 2. PL spectra of aliquots collected from ultrasonicated GO in 70% HNO_3 (red line) and under alkaline conditions (black line).

these PAH species is their ability to fluoresce around 390−420 nm, which agrees closely with the fluorescence detected from the filtered aliquots, for which we observed emission peaks at 410 nm. Figure 2 shows the photoluminescence spectra recorded from soluble molecular fragments dispersed in acidic or alkaline media. The solubility of these PAHs is pH-dependent, which would be expected from the presence of hydroxyl or carboxyl functional groups in these species. The solubility of these PAHs is lower under acidic conditions but increases under alkaline conditions. For this reason, we can see a widening of the emission spectral range in the alkaline medium in Figure 2.

One interesting observation is the peaking of the mass intensities with increasing sonication time followed by the decay of these intensities to baseline level. The initial increase in peak intensities was due to the kinetically controlled consumption of GO to form soluble precursors, which peaked at some time following the complete decomposition of the GO. With prolonged sonication time, the PAH molecules were kinetically converted into rolled-up carbon nanostructures that are more resistant to acid cutting, giving rise to a decay in the intensities of these species. The concentrated acid provided a dehydrating environment for the removal of hydroxyl groups from the edge sites of these polyaromatic molecules. Acid-catalyzed intramolecular or intermolecular dehydration reactions can occur between the edges of these PAHs to favor biaryl coupling and nucleation. The high energy density in cavitation allows intramolecular restructuring and nucleation to form fullerenes and CNTs. We speculate that once an initial seed structure forms, it can act as a kinetically controlled template for the assembly of PAHs, which favors subsequent molecular coupling and rearrangement into folded structures. The driving force for the assembly of these carbon structures is the preservation of internal π bonds. Figure 3 shows a schematic illustration of the proposed mechanism for the molecular reconstruction of PAH molecules into folded carbon nanostructures.

After sonication for some period of time, the concentration of PAHs in the solution decreased, and at that point, we could recover re-formed carbon nanostructures from the solution. The TEM images in Figure 4a−c show CNTs, fullerene-like carbon nanoparticles, and nanoribbons (see the Experimental Section). Figure 4a shows that the CNTs have outer diameters of 5−20 nm and lengths in the range 30−135 nm. The nanoribbons were obtained from the scission of GO sheets along their oxygen-decorated line defects.[10] The carbon nanoparticles and CNTs were reconstructed from molecular fragments of GO following its sonication and dissolution into PAHs. The TEM image in Figure 5a shows that a good yield of closed-end CNTs can be obtained. Figure 5b shows that the CNT walls are highly crystalline and that the inner diameters are 2−7 nm. The graphene sheets are aligned along the tube axis with an interwall spacing of 0.31 nm, consistent with the typical spacing in CNTs. All of the nanotubes have closed ends, indicating that small, soluble carbon precursors contribute to tube capping. If the tubes were formed from scrolling or curling of the GO nanosheets, open-ended tubes should be obtained instead.

Figure 6 shows Raman spectra of CNTs synthesized from GO, which are compared with those of SWNTs synthesized by chemical vapor deposition (CVD). The fingerprint modes due to CNTs (i.e., the tangential G band at 1581 cm^{-1} derived from the graphite-like in-plane mode and the disorder-induced D band at 1337 cm^{-1}) were clearly observed in both spectra.[11−14] Most importantly, the radial breathing modes (RBMs) between 100 and 300 cm^{-1} were also observed from the GO-derived CNT samples and were located in the same low-frequency range as the RBMs of SWNTs. The RBMs originate from radial expansion and contraction of the nanotubes, which are associated with vibrations of carbon atoms in a radial direction. This evidence proves the presence of CNTs.[15] According to the structure determination relationship between the RBMs and diameter, the diameter of the nanotubes was determined to be ∼1 nm, in agreement with results obtained by high-resolution TEM (HRTEM) and atomic force microscopy.

The fact that cavitation energy plays a key role in this process can be judged by increasing the temperature of the bath (>60 °C). In this case, although the global temperature was higher,

(10) Li, Z. Y.; Zhang, W. H.; Luo, Y.; Yang, J. L.; Hou, J. G. *J. Am. Chem. Soc.* **2009**, *131*, 6320.
(11) Dresselhaus, M. S.; Dresselhaus, G.; Jorio, A.; Souza, A. G.; Saito, R. *Carbon* **2002**, *40*, 2043.
(12) Jorio, A.; Saito, R.; Hafner, J. H.; Lieber, C. M.; Hunter, M.; McClure, T.; Dresselhaus, G.; Dresselhaus, M. S. *Phys. Rev. Lett.* **2001**, *86*, 1118.
(13) Rao, A. M.; Richter, E.; Bandow, S.; Chase, B.; Eklund, P. C.; Williams, K. A.; Fang, S.; Subbaswamy, K. R.; Menon, M.; Thess, A.; Smalley, R. E.; Dresselhaus, G.; Dresselhaus, M. S. *Science* **1997**, *275*, 187.
(14) Strano, M. S.; Doorn, S. K.; Haroz, E. H.; Kittrell, C.; Hauge, R. H.; Smalley, R. E. *Nano Lett.* **2003**, *3*, 1091.
(15) Seelaboyina, R.; Boddepalli, S.; Noh, K.; Jeon, M.; Choi, A. *Nanotechnology* **2008**, *19*, 065605.

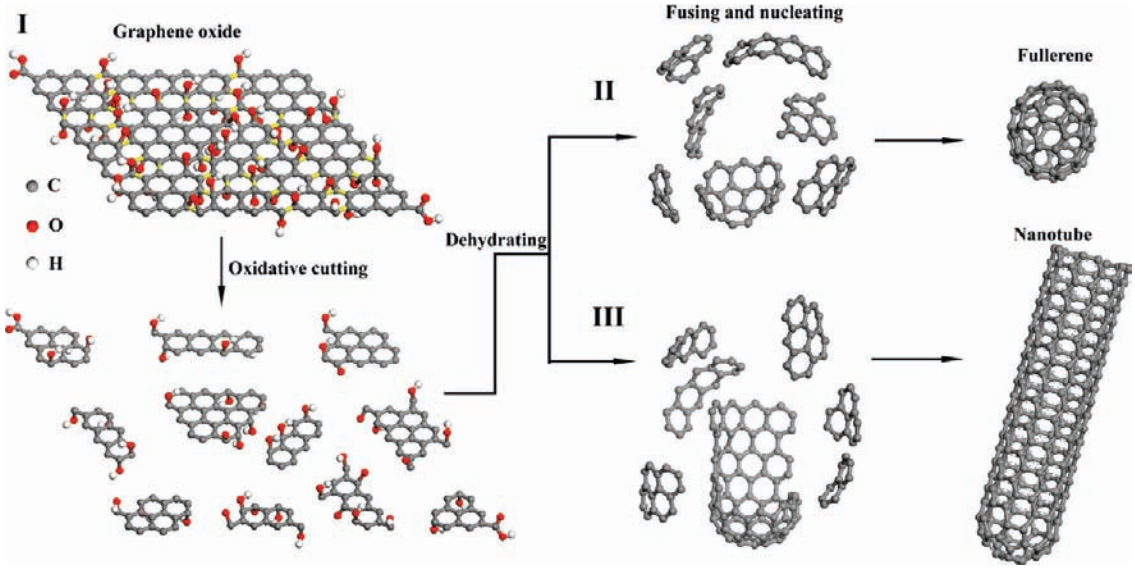

Figure 3. Schematic illustration of the mechanism for transforming GO nanosheets into carbon nanoparticles and nanotubes following their ultrasonication in acid. (I) Oxidative cutting of graphene oxide produces PAH molecules in concentrated HNO_3. In the dehydrating acidic medium, the polyaromatic fragments fuse and nucleate into (II) carbon nanoparticles or (III) nanotubes via acid-catalyzed intramolecular or intermolecular dehydration reactions.

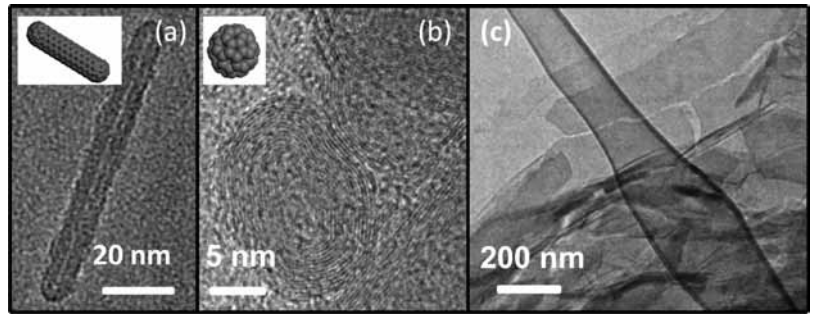

Figure 4. TEM images showing (a) a CNT, (b) carbon nanoparticles, and (c) nanoribbons obtained by sonicating GO sheets in 70% HNO_3 at RT.

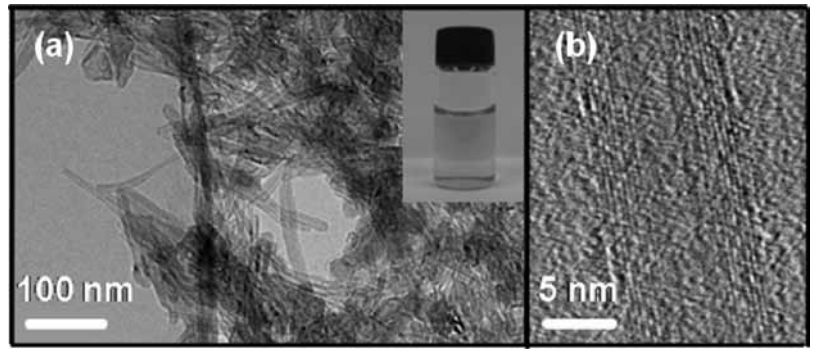

Figure 5. (a) TEM image showing CNTs obtained in good yield. The inset shows their water solubility. (b) HRTEM image of the tube walls of a CNT.

the energy density of cavitation decreased. As a result, at elevated temperature, we did not observe the formation of CNTs and obtained only fullerene-like carbon nanoparticles (Figure 7). These particles were found to be fluorescent at ~380 nm (Figure 7) and may belong to the same class of quantized carbon nanoparticles as that reported previously from the exfoliation of graphite rods.[16] At even higher temperatures in the sonication bath (>70 °C), the cavitation energy decreased drastically, and only poorly organized polyaromatic amorphous carbon was obtained.

XPS was applied to investigate the change in chemical composition of the GO upon sonication leading to formation of CNTs. Figure 8 shows the XPS spectra of GO and the synthesized CNTs. The GO spectrum shows peaks at 284.4, 286.3, and 288.7 eV, which correspond to C−C, C−O, and C(O)O chemical binding states, respectively. In the spectrum of CNTs, the peaks related to oxygenated carbon become visibly

(16) Zhou, J. G.; Booker, C.; Li, R.; Zhou, X. T.; Sham, T.-K.; Sun, X.; Ding, Z. F. *J. Am. Chem. Soc.* **2007**, *129*, 744.

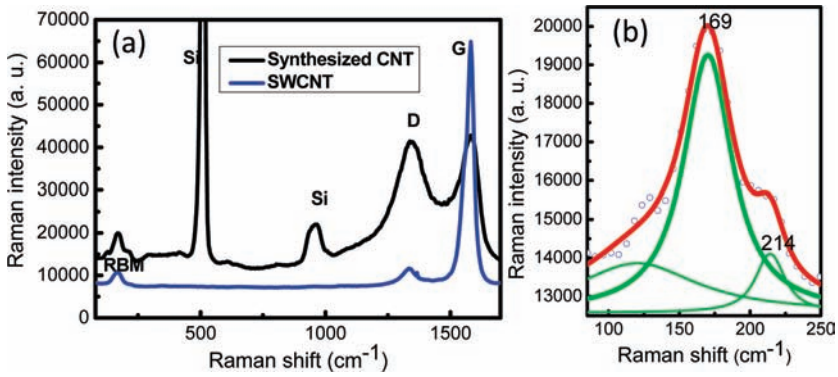

Figure 6. (a) Raman spectrum of CNTs synthesized from GO. The spectrum of commercially available SWNTs is shown for comparison. (b) Radial breathing modes of CNTs from GO and corresponding Lorenzian fits.

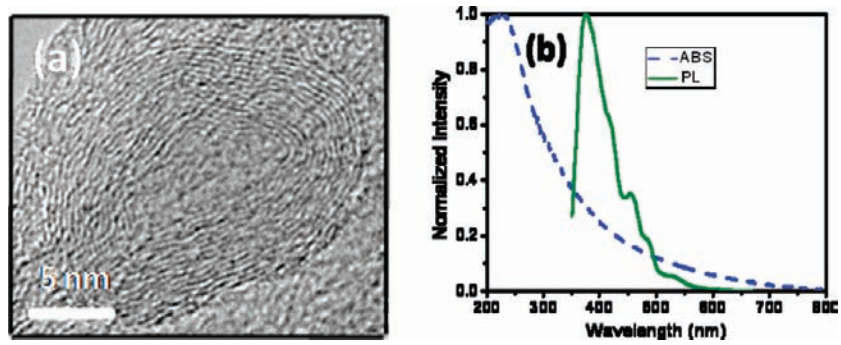

Figure 7. (a) HRTEM image of a carbon nanoparticle obtained by sonicating GO in 70% HNO_3 at 60 °C. (b) UV−vis absorption (ABS) and PL spectra of a aqueous carbon nanoparticle solution.

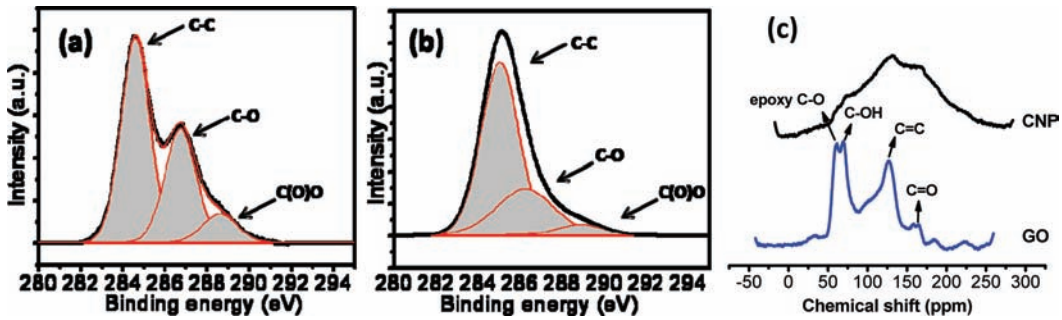

Figure 8. XPS spectra of (a) GO and (b) synthesized CNTs. (c) Solid-state ^{13}C MAS NMR spectra of GO and carbon nanoparticles (CNP) obtained by sonication of GO in 70% HNO_3 at 60 °C.

weakened. This indicates the occurrence of an acid-catalyzed dehydration mechanism that helps to transform the GO into reduced CNTs. A similar conclusion can be drawn from a solid-state NMR analysis of the formation of the carbon nanoparticles. Solid-state ^{13}C magic-angle-spinning (MAS) NMR spectroscopy was used to investigate the changes in chemical composition of GO upon sonication in acid at 60 °C. The spectrum of GO (Figure 8c) shows peaks at 134, 70, and 60 ppm, which correspond to unoxidized sp^2 carbons, hydroxylated carbons, and epoxidation, respectively.[17] The GO with a low degree of oxidation also has a resonance corresponding to carbonyl carbons at 167 ppm. After sonication, the peak intensity for the hydroxylated carbons relative to that for the sp^2 carbons was weakened significantly as a result of dehydration. In contrast, the peak intensity of the carbonyl carbons relative to the sp^2 carbons was enhanced. This can be explained by the cutting of GO along the edges or existing damage sites by HNO_3, leading to an increase in the number of carbonyl carbons.[10]

The CNTs obtained from this sonication process are generally quite short (aspect ratio <3). Quantum size effects cause finite CNTs to exhibit special properties such as magnetism.[18] The formation of localized edge states in finite-length CNTs with noncompensated zigzag open ends[19] has been predicted to promote magnetism. For graphene nanotubes, spin ordering may occur on the zigzag edges of hydrogen-terminated finite-sized carbon nanotubes. The magnetic ordering is sensitive to the tube index and geometry[20] and can range from antiferromagnetic-type to ferromagnetic-type ordering. Antiferromagnetic behavior reported in SWNTs is usually discussed in terms of an electronic

(17) Si, Y. C.; Samulski, E. T. *Nano Lett.* **2008**, *8*, 1679.

(18) Coskun, U. C.; Wei, T. C.; Vishveshwara, S.; Goldbart, P. M.; Bezryadin, A. *Science* **2004**, *304*, 1132.

(19) Okada, S.; Oshiyama, A. *J. Phys. Soc. Jpn.* **2003**, *72*, 1510.

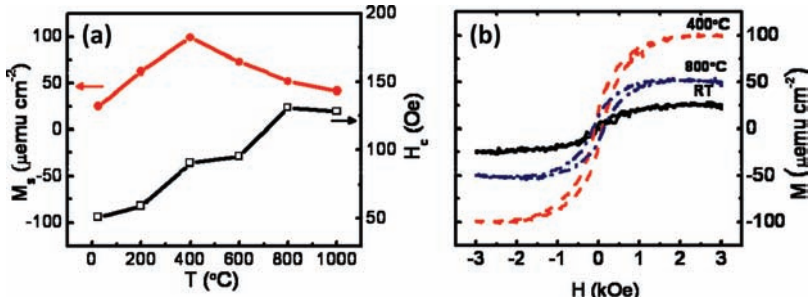

Figure 9. Magnetic properties of the CNTs. (a) Change in saturation magnetization and coercivity with annealing. (b) RT hysteresis curves after annealing at the indicated temperatures.

instability of the SWNTs or the occurrence of defect-mediated spin magnetism.[21]

Because of background interference from the ferromagnetic catalysts used in the CVD growth of CNTs, there is a limited number of experimental studies of the magnetic properties of CNTs. Unlike CNTs synthesized by CVD, the CNTs synthesized using GO as the precursor were not contaminated by any Ni or Co catalyst, and hence, intrinsic properties dominated the measurement. The saturation magnetization increased from 25 μemu cm^{-2} to a maximum of 100 μemu cm^{-2} upon annealing to 400 °C and gradually dropped to 41 μemu cm^{-2} on annealing at higher temperatures (Figure 9a). The coercive field increased with increasing annealing temperature and varied between 57 and 133 Oe. The origin of the ferromagnetism observed in these nanotubes is still not clearly understood. The closed ends of the nanotubes (Figure 4a) ruled out spin ordering in the zigzag edges of hydrogen-terminated finite-sized CNTs as the origin of the ferromagnetism. Instead, we suggest that broken conjugated graphenite structures were created via deoxidation of the basal plane during thermal annealing, and as a result, itinerant magnetism could arise from these defective graphenites through quasi-localized states induced at the Fermi level. Increased antiferromagnetic coupling and/or reconstruction of vacancy defects with further annealing resulted in the decline of the magnetic moments.

Conclusion

In summary, we have discovered a simple, low-energy route for transforming two-dimensional GO sheets into one-dimensional CNTs by ultrasonication of the GO nanosheets in concentrated acid at room temperature. The kinetically driven chemical transformation is almost magical in its "one-pot" transformation: the open, two-dimensional GO sheets, which are susceptible to acid cutting, can be readily decomposed into polyaromatics in concentrated acid in minutes. The polyaromatics are further reconstituted by acid dehydration reactions to form larger carbon nanoparticles and nanotubes. In other words, the net chemical transformation is from open-face carbon sheets to curled carbon nanostructures. From a technological viewpoint, the synthesis of water-soluble CNTs without the use of catalysts is advantageous because postsynthesis separation and purification processes are not needed. This method also generates novel carbon nanostructures arising from the unique growth environment. UV-emitting water-soluble carbon nanoparticles as well as short carbon nanotubes that exhibit magnetic properties can be fabricated. Most importantly, our experiments show that GO can be a good source of soluble PAHs for the liquid-phase synthesis of carbon nanostructures. The discovery that PAHs can be reconstituted into carbon nanostructures by sonication in acids has wide implications for carbon conservation and transformation. Solution processing of polyaromatics using GO as the starting precursor, in combination with separation and isolation of species, may afford a new route to the synthesis of graphene-like molecules.

Acknowledgment. We thank NRF-CRP for support (Grant "Graphene Related Materials and Devices" R-143-000-360-281).

JA905968V

(20) Chen, R. B.; Chang, C. P.; Hwang, J. S.; Chuu, D. S.; Lin, M. F. *J. Phys. Soc. Jpn.* **2005**, *74*, 1404.
(21) Likodimos, V.; Glenis, S.; Guskos, N.; Lin, C. L. *Phys. Rev. B* **2007**, *76*, 5.